Physica A 461 (2016) 778–787

Contents lists available at ScienceDirect

Physica A

journal homepage: www.elsevier.com/locate/physa

The trading time risks of stock investment in stock price drop☆

Jiang-Cheng Li [a,b], Nian-Sheng Tang [a,*], Dong-Cheng Mei [c], Yun-Xian Li [a,b], Wan Zhang [b]

[a] Department of Statistics, Yunnan University, Kunming 650091, PR China
[b] School of Finance, Yunnan University of Finance and Economics, Kunming 650221, PR China
[c] Department of Physics, Yunnan University, Kunming 650091, PR China

HIGHLIGHTS

- We empirically investigate the trading time risk (TTR) of stock investment via escape time in ˆDJI and CSI300.
- A peak distribution for shorter trading days and a two-peak distribution are observed.
- There is the monotonicity (or non-monotonicity) for the stability of the absolute (or relative) TTR.
- The trading day plays an opposite role on the absolute (or relative) TTR and its stability between ˆDJI and CSI300.

ARTICLE INFO

Article history:
Received 12 October 2015
Received in revised form 21 April 2016
Available online 11 June 2016

Keywords:
Escape time
Financial markets
Stability
Stock investment
Time risk

ABSTRACT

This article investigates the trading time risk (TTR) of stock investment in the case of stock price drop of Dow Jones Industrial Average (ˆDJI) and Hushen300 data (CSI300), respectively. The escape time of stock price from the maximum to minimum in a data window length (DWL) is employed to measure the absolute TTR, the ratio of the escape time to data window length is defined as the relative TTR. Empirical probability density functions of the absolute and relative TTRs for the ˆDJI and CSI300 data evidence that (i) whenever the DWL increases, the absolute TTR increases, the relative TTR decreases otherwise; (ii) there is the monotonicity (or non-monotonicity) for the stability of the absolute (or relative) TTR; (iii) there is a peak distribution for shorter trading days and a two-peak distribution for longer trading days for the PDF of ratio; (iv) the trading days play an opposite role on the absolute (or relative) TTR and its stability between ˆDJI and CSI300 data.

1. Introduction

Econophysics is a new branch of physics, which uses physical ideas and methods to study economic or financial problems [1,2]. Theories of econophysics present some new explanations for classical financial problems such as market data of peak fat-tail characteristic [3,4], long range memory and clustering of volatility [5]. For example, Mantegna & Stanley [2],

☆ This work was supported by the grants from the National Science Fund for Distinguished Young Scholars of China (Grant No.: 11225103), the National Natural Science Foundation of China (Grant No.: 11165016), the China Postdoctoral Science Foundation (Grant No.: 2015M572507), the program of IRTSTYN in Yunnan province and the Science Foundation of Yunnan University (Grant No.: 2009A001Z).
* Corresponding author.
E-mail address: nstang@ynu.edu.cn (N.-S. Tang).

http://dx.doi.org/10.1016/j.physa.2016.06.064

Gopikrishnan et al. [6] and Malevergne et al. [7] portrayed the financial asset prices for various time scales of statistical features, and explained commendably the peak fat-tail characteristics by using the stable Lévy distribution [5,8], power-law tail distribution, and tensile index distribution, respectively; Peters [9] used the chaos and fractal theory to study the financial markets, and proposed the fractal market hypothesis that is different from the efficient market hypothesis [10]; Mantegna & Stanley [2] employed the probability theory, critical phenomena in physics and turbulence theory to analyze financial time series, and proposed a new stochastic model; Bouchaud et al. [11] adopted the method of statistical physics to empirically investigate statistical characteristics of financial prices, and threw doubt on the rationality of the central limit theorem for the cornerstone of the classical financial risk theory. On the other hand, physicists studying the financial system broadened the research field of the traditional finance. For example, Mandelbrot [12] pointed out that the Wall Street stock market data present multi scale fractal features; Jiang & Zhou [13] and Yuan & Zhuang [14] found the universality of multi scale fractal phenomenon in studying China's capital market; Huang [15] in the "Physics Reports" systematically elaborated the experimental econophysics concerned with statistical physics of humans in the laboratory. This is based on the controlled human experiments developed by physicists for studying some economic or financial problems. In addition, the escape time as a physical quantity has been widely used in various fields such as chemical reaction system [16,17], gene expression dynamics [18], stochastic resonance phenomenon in a vegetation ecological system [19]. Also, the noise enhanced stability phenomenon is observed by the method of escape time [20–22]. For example, Dubkov et al. [20] found the noise enhanced stability phenomenon in a piece-wise linear dichotomously fluctuating potential with metastable state; Spagnolo, Agudov and Dubkov [21] experimentally and numerically discussed the noise enhanced stability in different physical systems; Spagnolo et al. [22] reviewed the noise enhanced stability and the resonant activation for models of interdisciplinary physics. The escape time can be usually employed to describe the stability of stochastic system, e.g., in a stochastic single-gene network [23], active Brownian motion [24] and an ecological system [25]. Soon afterwards, since a Langevin equation approach to a model for stock market fluctuations and crashes was proposed [26], the stock price escape phenomenon in stock market crashes has been widely discussed. For example, Valenti et al. [27] and Spagnolo and Valenti [28] investigated statistical properties of the hitting times for stock market evolution for several models, Masoliver and Perellö [29,30] presented exact expressions for the survival probability and the mean exit time, Bonanno et al. [31,32] studied the mean escape time for financial markets, Bonanno & Spagnolo [33] discussed escape times of stock price returns for the Wall Street market, and Li and Mei [34] and Li et al. [35] analyzed the returns and risks of investment.

Risk of stock investment is widely studied by investors and scholars [31,32,34–41]. For example, Markowitz [36,37] developed the mean–variance model for risk of stock investment in which mean was used to represent the expect return and variance was employed to measure the risk; Turner, Startz & Nelson [38] discussed the heteroskedasticity, risk and learning in the stock market via a Markov model; Lo & Repin [39] observed significant differences among physiological responses across 10 traders in discussing the psychophysiology of real-time financial risk processing; Tang & Tsitsiashvili [40] discussed the ruin probability of the finite horizon in a discrete-time model with heavy-tailed insurance and financial risks; Christoffersen [41] investigated the elements of financial risk management; Bonanno, Valenti & Spagnolo [31,32] used the Heston model and mean escape time to discuss the returns and risks in stock market crashes. Hence, risk of stock investment in a financial market is worthy to be further investigated.

The main purpose of this paper is to discuss the trading time risk (TTR). If the time of the stock price from high to low is shorter in the case of stock price drop, the time of investors to trade their stocks is less. In this case, investors will face a higher TTR. In particular, in the case of stock market crashes, investors lack the time to sell their stocks in the region of the right price. In other words, an increase of TTR for investors trading in stock price drop leads to a decrease of time from high to low (i.e., the escape time). Hence, to investigate the TTR, we here employ the escape time [31,32,34,35] to calculate the time of the stock price from high to low. Also, we investigate the TTRs of stock investment for the Dow Jones Industrial Average (ˆDJI) and Hushen300 (CSI300) data.

The rest of this paper is organized as follows. Section 2 presents a model of the TTR in the case of stock price drop based on the escape time [31,32,34,35]. Section 3 investigates statistical properties of TTR. Section 4 presents a theoretical model. Some discussions are given in Section 5.

2. The trading time risks in stock price drop

If the time of the stock price from high to low is shorter in the case of stock price drop, the time of selling stock for investors is less. In this case, investors will face a higher risk. In particular, when the stock market crashes, investors lack the time to sell their stock in a reasonable price range, i.e., when stock price drops, the time decrease from high to low leads to an increase of investors' TTR. Hence, to investigate the TTR, we employ the escape time [31,32,34,35] to calculate the time of the stock price from high to low.

A real stock price is a stochastic time series with respect to the data selection period (e.g., 1 min, 1 h, 1 day, ...). Let $P_1, P_2, \ldots$ be a stock price time series. To find the maximum and minimum values of N data periods at the tth point-in-time, we take $N_{\text{max-min}}$ periods before the tth time point (including the tth time point) to be a data window in calculating the following maximum and minimum values of $N_{\text{max-min}}$ periods:

$$P^{\max}_{t,N_{\text{max-min}}} = \text{Max}\{P_{t-N_{\text{max-min}}}, P_{t-N_{\text{max-min}}+1}, \ldots, P_{t-1}, P_t\},$$
$$P^{\min}_{t,N_{\text{max-min}}} = \text{Min}\{P_{t-N_{\text{max-min}}}, P_{t-N_{\text{max-min}}+1}, \ldots, P_{t-1}, P_t\}.$$

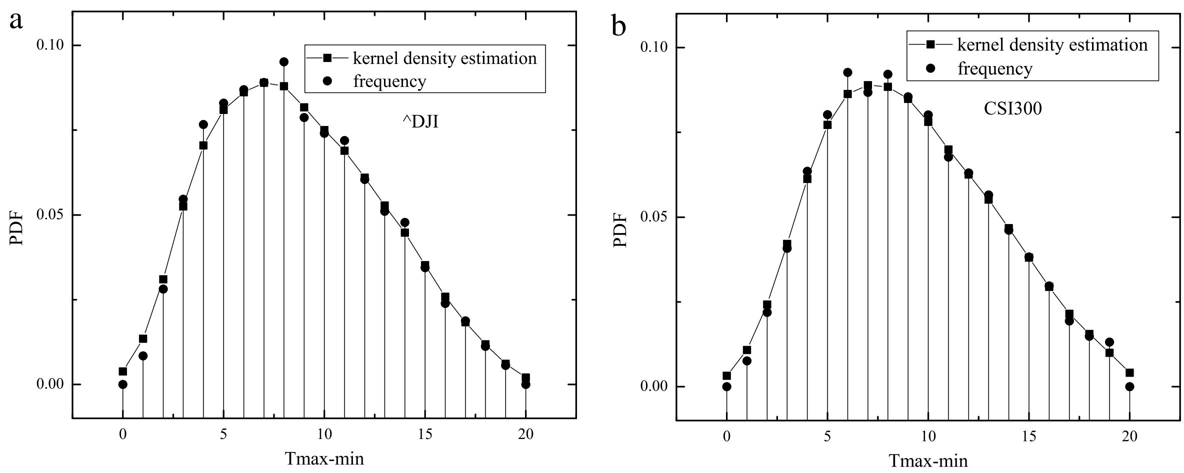

Fig. 1. Probability density function (PDF) of escape time $T_{\text{max–min}}$ via frequency and kernel density estimation methods with $N_{\text{max–min}} = 20$ and 1 trading day being data period for the ˆDJI data (left panel) and CSI300 data (right panel).

Let $t_t^{\max}$ and $t_t^{\min}$ be the point-in-times of data window $\{P_{t-N_{\text{max–min}}}, \ldots, P_t\}$, which are equal to $P^{\max}_{t,N_{\text{max–min}}}$ and $P^{\min}_{t,N_{\text{max–min}}}$, respectively. Considering a stock price drop process, the stock price of the $N_{\text{max–min}}$ periods will make a record low and then maximum value also can become low. Therefore, we consider the following three conditions:

(1) a record low comes first, i.e., $t_t^{\max} < t_t^{\min}$;
(2) a record low, i.e., $t_{t-1}^{\min} < t_t^{\min}$;
(3) a record high comes before the stock price drop, i.e., $t_{t-1}^{\min} < t_t^{\max}$.

Then, we can obtain the escape time $T_{\text{max–min}}$ of stock price from the maximum $P^{\max}_{t,N_{\text{max–min}}}$ to minimum $P^{\min}_{t,N_{\text{max–min}}}$ for $N_{\text{max–min}}$ periods. Obviously, the escape time is $T_{\text{max–min}} = t_t^{\min} - t_t^{\max}$ for the above considered three conditions. Also, the TTR is inversely proportional to the escape time $T_{\text{max–min}}$. In what follows, we discuss probability density function (PDF) of TTR for two real financial markets, and call the risk defined by the escape time $T_{\text{max–min}}$ as the absolute TTR.

3. The probability density function

To empirically investigate the performance of the absolute TTR, we calculate the PDF of the escape time $T_{\text{max–min}}$ for a real data set. Also, to investigate the effect of the data on the performance of the absolute TTR, we consider the adjusted close prices in two markets. One is 30 stocks in Dow Jones Industrial Average (ˆDJI) from 29 march 1990 (or offering date) to 3 June 2013 [42]. The other one is 300 stocks in HuShen 300 (CSI300) index from 4 January 2000 (or offering date) to 4 April 2015 [43].

The PDFs of the escape time $T_{\text{max–min}}$ for the ˆDJI and CSI300 data are plotted in Fig. 1(a) and (b), respectively. Also, we calculate their corresponding kernel density estimations [44–46], which are given in Fig. 1(a) and (b), respectively. Here, the bandwidth is taken to be a unit period of the escape time. Examination of Fig. 1 indicates that (i) there is a peak value for PDF of $T_{\text{max–min}}$; (ii) there is a high consistence between the empirical estimation and the kernel density estimation. Hence, the following results are obtained via the kernel density estimation.

The PDFs of the escape time $T_{\text{max–min}}$ with different values of $N_{\text{max–min}}$ for the ˆDJI data and CSI300 data are presented in Fig. 2(a) and (b), respectively, which shows a peak distribution. Inspection of Fig. 2 indicates that the maximum value of distribution first decreases and then increases as $N_{\text{max–min}}$ increases. Also, $T_{\text{max–min}}$ corresponding to the peak first moves to a longer escape time and then moves to a shorter escape time. In addition, we calculate the expectation and standard deviation of the ˆDJI and CSI300 data corresponding to Fig. 2, which are shown in Table 1. Examination of Table 1 indicates that (i) the expectations of the ˆDJI and CSI300 data increase as $N_{\text{max–min}}$ increases; (ii) standard deviation increases as $N_{\text{max–min}}$ increases, i.e., there is the monotonicity for the expectation and standard deviation of the escape time as a function of $N_{\text{max–min}}$. The above findings show that increasing the data window length $N_{\text{max–min}}$ leads to a decrease of the absolute TTR due to the fact that the longer the expectation of the escape time $T_{\text{max–min}}$, the weaker the absolute TTR ; increasing standard deviation weakens the stability of the absolute TTR due to the longer standard deviation of the escape time $T_{\text{max–min}}$.

The PDFs of the escape time $T_{\text{max–min}}$ with various trading days for the ˆDJI and CSI300 data are given in Fig. 3(a) and (b), respectively. Examination of Fig. 3 shows a peak distribution for shorter trading days (e.g., trading days = 5) and a two-peak distribution for longer trading days (e.g., trading days = 30). Also, Fig. 3(a) indicates that increasing the trading days enhances the maximum peak, but Fig. 3(b) implies that the peak of distribution first decreases and then increases. Again, the expectations and standard deviations of the ˆDJI and CSI300 data are presented in Table 2, which shows that the expectation of the ˆDJI data decreases but the expectation of the CSI300 data increases as the trading day increases. On the

Table 1
Expectations and standard deviations (SD) of the ˆDJI and CSI300 data for various $N_{max-min}$.

$N_{max-min}$	ˆDJI data		CSI300 data	
	Expectation	SD	Expectation	SD
10	4.682	2.040	4.805	2.039
30	8.630	4.018	8.977	4.094
60	23.55	11.25	25.64	12.91
120	44.52	23.83	48.38	27.22
200	65.84	40.04	76.61	47.50

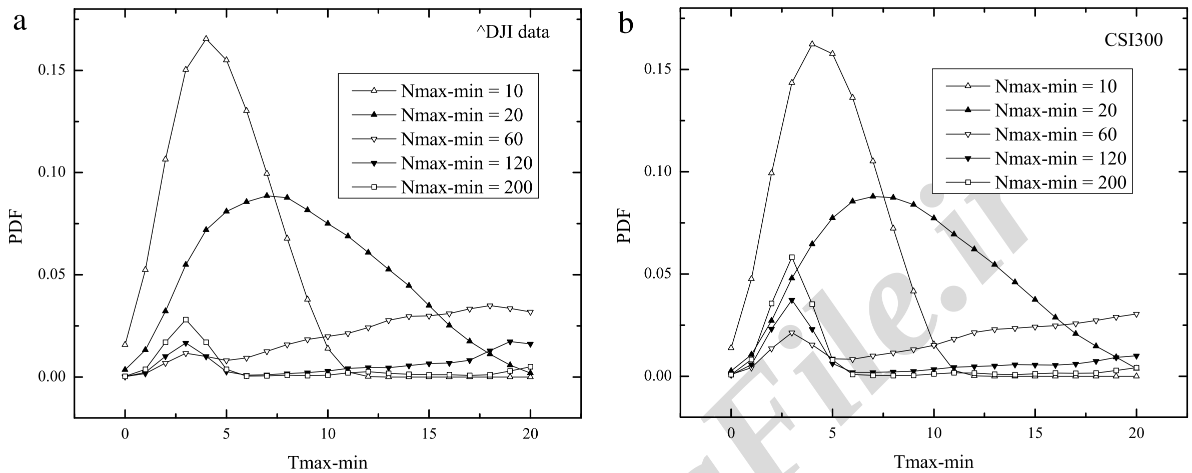

Fig. 2. Probability density function (PDF) of escape time $T_{max-min}$ at 1 trading day under different values of $N_{max-min}$ for the ˆDJI data (left panel) and CSI300 data (right panel).

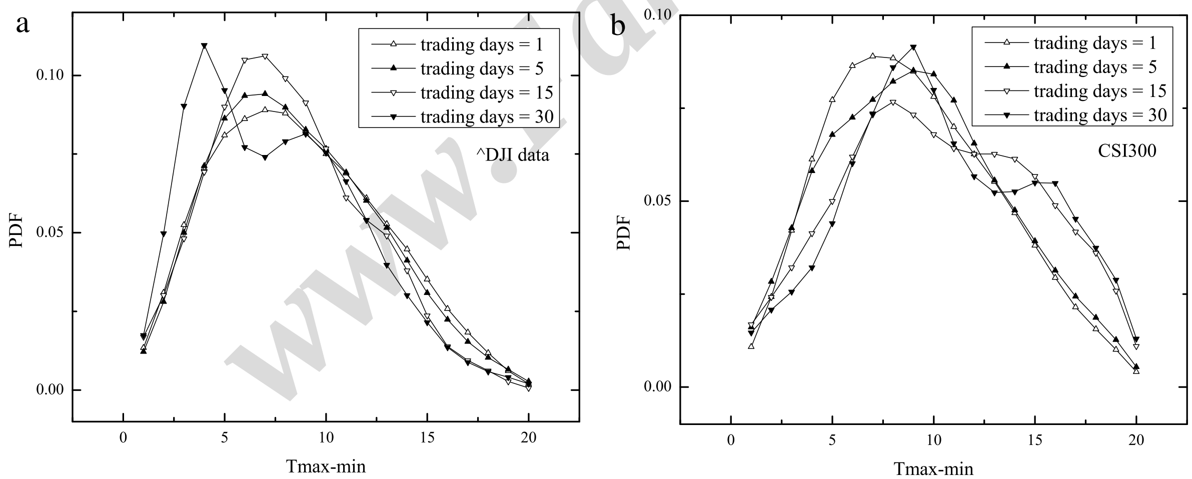

Fig. 3. Probability density function (PDF) of escape time $T_{max-min}$ at $N_{max-min} = 20$ under different trading days for the ˆDJI data (left panel) and CSI300 data (right panel).

other hand, Fig. 3(a) shows that increasing the trading days first weakens the standard deviation and then enhances the standard deviation, i.e., a maximum stability of the absolute TTR for the ˆDJI data is consistent with the optimal trading days (e.g., trading days = 15); while Fig. 3(b) implies that the standard deviation first enhances and then weakens as the trading day increases, i.e., a minimum stability of the absolute TTR for the CSI300 data is consistent with the worst trading days (e.g., trading days = 15). That is, the non-monotonicity is observed in terms of the expectation and standard deviation of the escape time as a function of the trading days. From a perspective of financial, increasing the trading days enhances the absolute TTR for the ˆDJI data, but weakens the absolute TTR for the CSI300 data. The above observations show that increasing the trading days play an opposite effect on the absolute TTR and the stability between ˆDJI and CSI300.

Table 2
Expectations and standard deviations (SD) of the ˆDJI and CSI300 data for various trading days.

Trading days	ˆDJI data		CSI300 data	
	Expectation	SD	Expectation	SD
1	8.683	4.033	9.078	4.091
5	8.574	3.933	9.247	4.272
15	8.113	3.658	10.29	4.686
30	7.644	3.878	10.49	4.602

Table 3
Expectations and standard deviations (SD) of the ˆDJI and CSI300 data for various $N_{max-min}$.

$N_{max-min}$	ˆDJI data		CSI300 data	
	Expectation	SD	Expectation	SD
10	0.4682	0.2040	0.4823	0.2048
30	0.4315	0.2009	0.4538	0.2011
60	0.3925	0.1875	0.4483	0.2080
120	0.3710	0.1987	0.4077	0.2080
200	0.3292	0.2002	0.3795	0.2167

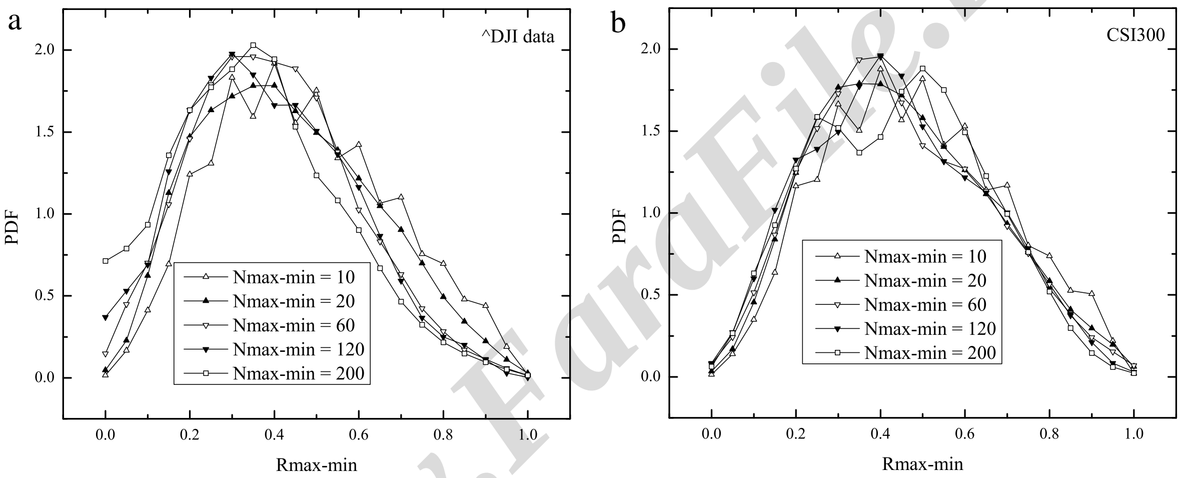

Fig. 4. Probability density function (PDF) of the relative rate of escape time $R_{max-min}$ at 1 trading day under different values of $N_{max-min}$ for the ˆDJI data (left panel) and CSI300 data (right panel).

Due to the correlation between $T_{max-min}$ and $N_{max-min}$, it is rather difficult to compare the values of TTR for various $N_{max-min}$. Hence, we employ the relative escape time ratio $R_{max-min} = T_{max-min}/N_{max-min}$ to measure the relative TTR with different data windows. The PDFs of the relative escape time ratio $R_{max-min}$ with various $N_{max-min}$ for the ˆDJI and CSI300 data are plotted in Fig. 4(a) and (b), respectively. Fig. 4 indicates a peak distribution, but it is rather difficult to identify the graphic details due to the insufficient sample and small bandwidth (1/20). Hence, we calculate the expectation and standard deviation of the ˆDJI and CSI300 data, which are shown in Table 3. Examination of Table 3 implies that the expectations of the ˆDJI and CSI300 data monotonically decrease, but their corresponding standard deviations first decrease and then increase as $N_{max-min}$ increases. In other words, there is a monotonicity in terms of the expectation of $R_{max-min}$ and a non-monotonicity in terms of the standard deviation of $R_{max-min}$ for various values of $N_{max-min}$. From a perspective of financial, increasing the data window length $N_{max-min}$ leads to a decrease of the relative TTR. Also, the minimum of standard deviations is consistent with the maximum stability of the relative TTR for the ˆDJI and CSI300 data. The above findings show that $N_{max-min}$ has the same effect on the relative TTR and the stability between ˆDJI and CSI300.

The PDFs of the relative escape time ratio $R_{max-min}$ with different trading days for the ˆDJI and CSI300 data are presented in Fig. 5(a) and (b), respectively. The bandwidth in Fig. 5 is the same as that in Fig. 4. Fig. 5 shows a peak distribution for shorter trading days (e.g., trading days = 5) and a two-peak distribution for longer trading days (e.g., trading days = 30). From Fig. 5(a), increasing trading days enhances the maximum peak, but it follows from Fig. 5(b) that distribution first decreases and then increases. Also, we calculate the expectations and standard deviations of $R_{max-min}$ for the ˆDJI and CSI300 data, which are shown in Table 4. From Table 4, the expectation of $R_{max-min}$ decreases for the ˆDJI data but increases for the CSI300 data as the trading day increases. Increasing the trading days first weakens the standard deviation and then enhances the standard deviation for the ˆDJI data, but first enhances the standard deviation and then weakens the standard deviation for

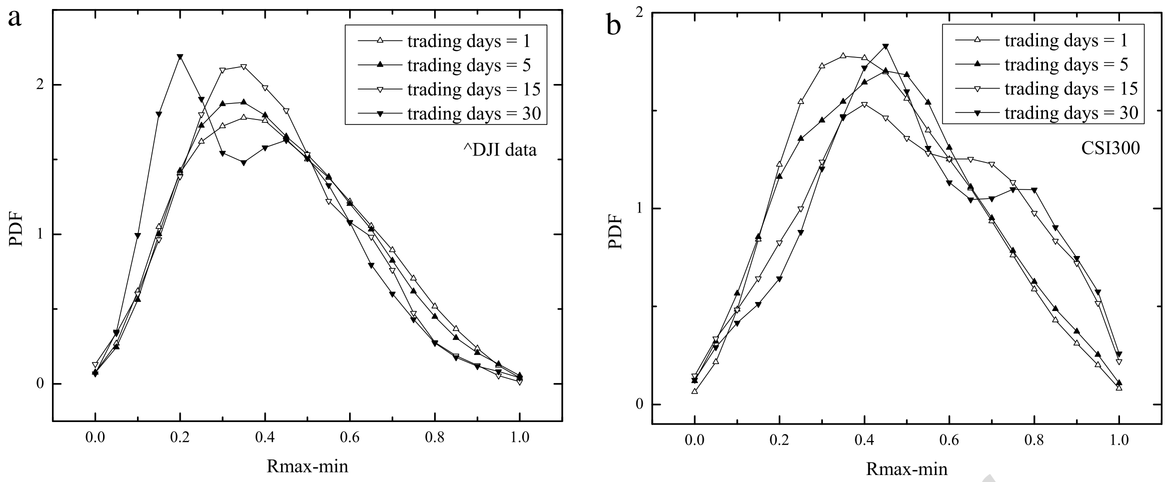

Fig. 5. Probability density function (PDF) of the relative rates of escape time $R_{max-min}$ at $N_{max-min} = 20$ under different trading days for the ˆDJI data (left panel) and CSI300 data (right panel).

Table 4
Expectations and standard deviations (SD) of the ˆDJI and CSI300 data for various trading days.

Trading days	ˆDJI data		CSI300 data	
	Expectation	SD	Expectation	SD
1	0.4342	0.2016	0.4539	0.2045
5	0.4287	0.1966	0.4623	0.2136
15	0.4056	0.1829	0.5148	0.2343
30	0.3822	0.1939	0.5247	0.2301

the CSI300 data, i.e., the maximum (or minimum) stability of the relative TTR for the ˆDJI (or CSI300) data is consistent with the optimal (or worst) trading days (e.g., trading days = 15). In other words, the expectation (or standard deviation) of $R_{max-min}$ is a monotone (or non-monotone) function of $N_{max-min}$. From the perspective of financial, increasing the trading days enhances the relative TTR for the ˆDJI data, but weakens the relative TTR for the CSI300 data. The above observations show that increasing the trading days has an opposite effect on the absolute TTR and the stability between ˆDJI and CSI300.

Finally, to examine the rationality of estimation of two-peak distribution in Figs. 3 and 5, the PDFs at 30 trading days in Figs. 3(a), (b), 5(a) and (b) are calculated by frequency and kernel density estimation methods plotted in Fig. 6(a), (b), (c) and (d), respectively. The bandwidth is taken to be a unit trading day in Fig. 6(a) and (b), which is the same as in Fig. 3, and the bandwidth in Fig. 6(c) and (d) is the same as that in Fig. 5. Also, two methods show the two-peak distribution. Hence, the previous results are rational via the kernel density estimation. From a financial point of view, the performance of two-peak distribution results from the diversity and different classification of the stocks in market. Industry, public utilities, medical, computer and other varieties of stocks are included in the stock market. According to the performance of the company, the stocks can be simply divided into junk stocks with poor performance and blue chips with better performance. Obviously, in stock market crashes after its bubble, the stock prices fall relatively slowly for blue chips due to the stable value of blue chips, but decrease faster for junk stocks due to the unstable value of junk stock. In Fig. 6 with the same conditions, the blue chips tend to have a longer escape time, but junk stocks generally have a shorter escape time. This is a reason for a behavior of two-peak distribution observed in Fig. 6.

4. The model

In Refs. [20–22,31], the escape time is shown to have the characteristic of exponential function using the theoretical and empirical methods. Thus, the escape time $T_{max-min}$ can be defined as

$$T_{max-min} = A \exp\left(\frac{\Delta V}{\upsilon}\right), \quad (1)$$

where A represents a prefactor which depends on the potential profile, ΔV is a barrier, and υ is the noise intensity. From the perspective of physics, the escape time is the time that a Brownian particle with a noise intensity moves throughout a barrier ΔV. In a financial market, the noise intensity υ and barrier ΔV are directly related to investors and stocks. The utility of investors on the returns and risks of stocks affects their trading behaviors. When the utilities of investors move throughout their barriers of utilities, investors escape from market and stock will crash from high to low. Hence, $\Delta V/\upsilon$ is

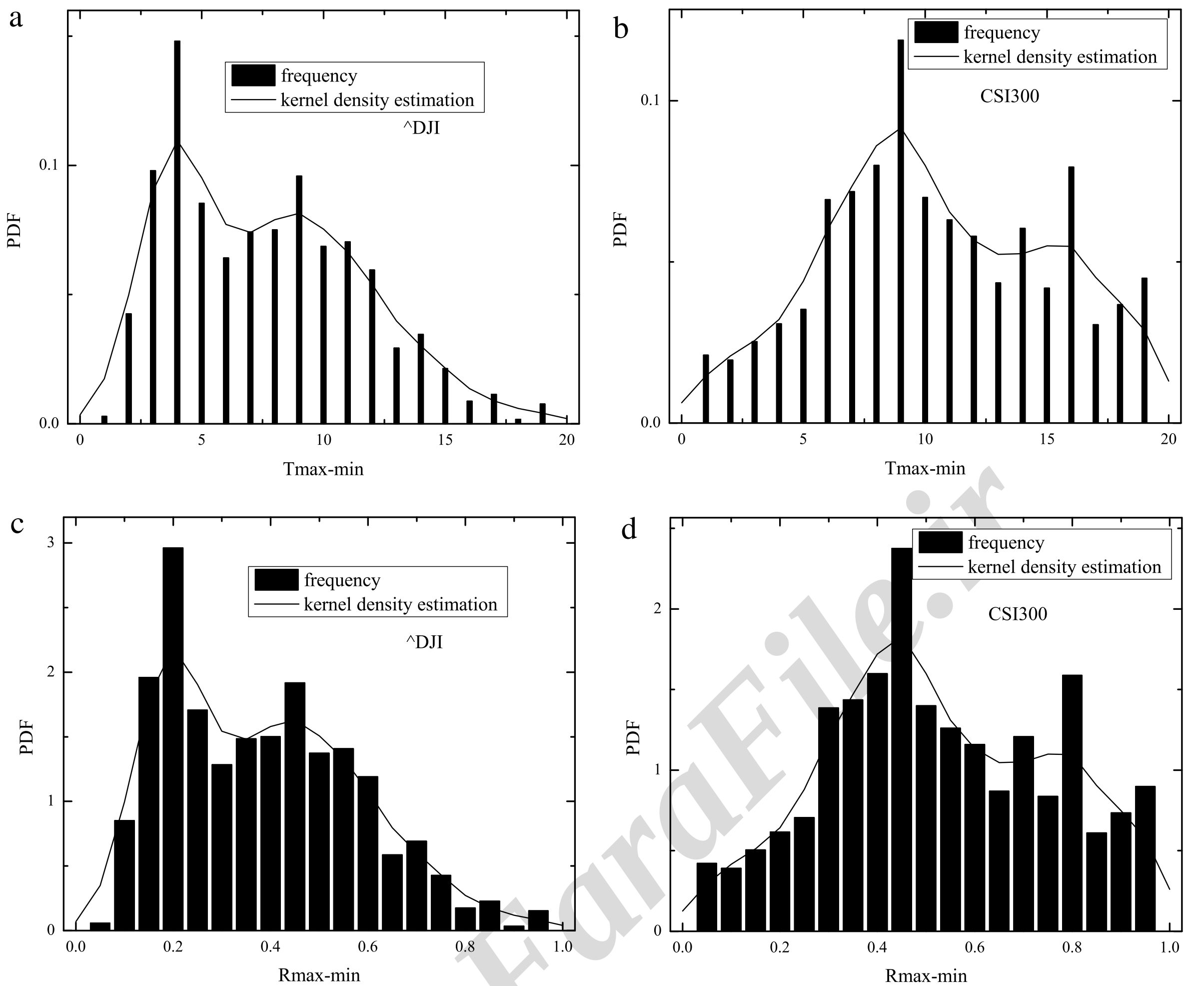

Fig. 6. Probability density function (PDF) of escape time $T_{\text{max-min}}$ (or $R_{\text{max-min}}$) via frequency and kernel density estimation methods with 30 trading days being the data period for the ˆDJI data in (a) (or (c)) and CSI300 data (b) (or (d)).

concerned with the utilities of investors. The utility function is related to return r and its mean μ and variance σ^2 [47]. Finally, a potential function $U(r, \mu, \sigma^2, N_{\text{max-min}})$ is analogous to a utility function and is employed to replace $\Delta V/\upsilon$. Thus, Eq. (1) can be written as

$$T_{\text{max-min}} = A \exp\{U(r, \mu, \sigma^2, N_{\text{max-min}})\}. \tag{2}$$

The return r is stochastic, and the PDF of return can be obtained by the following Gaussian kernel density [44–46]

$$P_r(r) = \frac{1}{\sqrt{2\pi}nh} \exp\left\{-\frac{1}{2}\sum_{i=1}^{n}\left(\frac{r-r_i}{h}\right)^2\right\}, \tag{3}$$

where r_i is the ith sample observation of return r, n is the total number of samples, h is the bandwidth. For the case that $N_{\text{max-min}} = 20$ and $h = 0.01$, the PDFs of return at 1 and 30 trading days for the ˆDJI and CSI300 data are shown in Fig. 7(a) and (b) [48,49], respectively. From Fig. 7, we observe that $|r|$ is less than 1 in most cases, the peak value for the PDF of return is close to zero. For the given total number of samples, μ and σ^2 can be estimated by their corresponding sample mean and sample variance, respectively. For simplicity, μ and σ^2 are considered as a constant at a given total number of samples. Taking the first-order Taylor expansion of $U(r|\mu, \sigma^2, N_{\text{max-min}})$ at $r = 0$ yields

$$U(r|\mu, \sigma^2, N_{\text{max-min}}) = a_0 + a_1 r + O(r^2), \quad |r| \le 1, \tag{4}$$

where a_0 and a_1 are the coefficients when μ, σ^2 and $N_{\text{max-min}}$ are given. Hence, the function of return with respect to the escape time $T_{\text{max-min}}$ is given by

$$r = h(T_{\text{max-min}}) \simeq \frac{U(r|\mu, \sigma^2, N_{\text{max-min}}) - a_0}{a_1} = \frac{\log\left(\frac{T_{\text{max-min}}}{A}\right) - a_0}{a_1}. \tag{5}$$

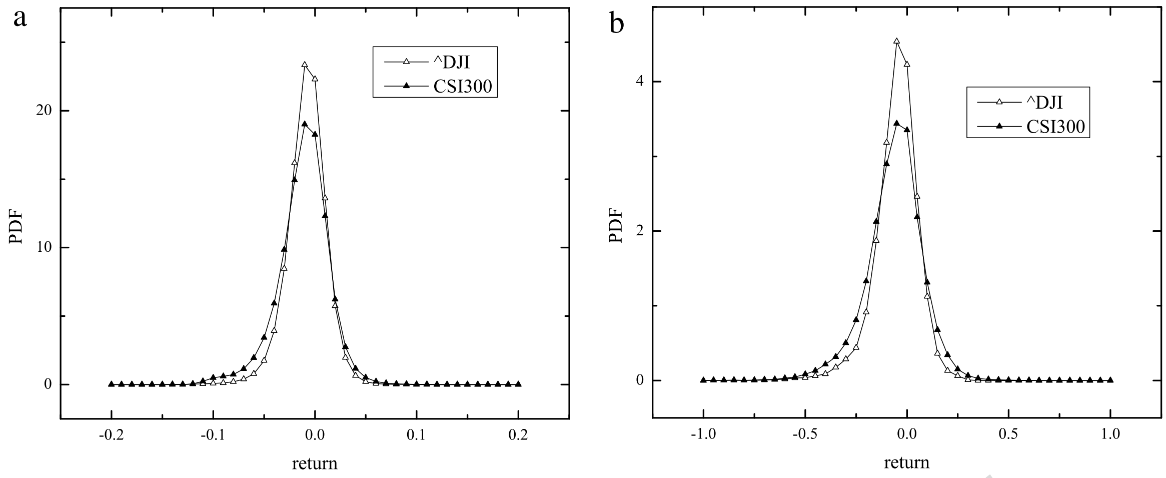

Fig. 7. Probability density function (PDF) of return via kernel density estimation methods with $N_{\max-\min} = 20$ at 1 trading day in (a) and 30 trading days in (b).

Finally, from Eqs. (3) and (5), we obtain the following PDF of $T_{\max-\min}$:

$$P_T(T_{\max-\min}) = P_r(h(T_{\max-\min}))|h'(T_{\max-\min})|$$
$$= \frac{1}{\sqrt{2\pi}nha_1T_{\max-\min}} \exp\left\{-\frac{1}{2}\sum_{i=1}^{n}\left(\frac{\frac{\log\left(\frac{T_{\max-\min}}{A}\right)-a_0}{a_1}}{h} - r_i\right)^2\right\},$$

where $h'(\cdot)$ is the first derivative of function $h(\cdot)$. Finally, from the above equation, the average TTR (e.g., $E(T_{\max-\min})$) can be evaluated by

$$E(T_{\max-\min}) = \int_0^{\infty} T_{\max-\min}P_T(T_{\max-\min})\mathrm{d}T_{\max-\min}.$$

To compare the above theoretical model and the empirical results given in Section 3, the PDFs of the escape time $T_{\max-\min}$ corresponding to frequency estimation (e.g., see Fig. 1) and theoretical result for the ˆDJI and CSI300 data are plotted in Fig. 8(a) and (b), respectively. Here, the theoretical result for the ˆDJI data is computed by setting $A = 3.767$, $a_0 = 0.852$ and $a_1 = 0.585$; while the theoretical result for the CSI300 data is evaluated by taking $A = 5.976$, $a_0 = 0.435$ and $a_1 = 0.5525$. Fig. 8 shows that there is a good consistence between frequency estimation and theoretical result. Also, the theoretical average TTRs in Fig. 8(a) and (b) are 8.735 and 9.169, respectively, which are rather close to their corresponding empirical values (e.g., see Table 2). For the longer trading days (e.g., 30 trading days), Fig. 9 plots the PDFs of the escape time $T_{\max-\min}$ with $N_{\max-\min} = 20$ for frequency of real data and theoretical result. Here, the theoretical result for the ˆDJI data is calculated by setting $A = 2.51$, $a_0 = 1.11$ and $a_1 = 0.6737$; the theoretical result for the CSI300 data is evaluated by taking $A = 4.195$, $a_0 = 1.007$ and $a_1 = 0.5089$. The theoretical average TTR values in Fig. 9(a) and (b) are 7.382 and 9.552, respectively, which are quite close to their corresponding empirical values (e.g., see Table 2). Examination of Fig. 9 shows that there is a relatively good consistence between the real data and the theoretical result. The above results show that increasing the trading days (e.g., from Fig. 8 to Fig. 9) leads to an increase of the discrepancy between the empirical and theoretical distributions, which is consistent with that observed in Refs. [50,51].

5. Conclusions

To investigate the TTR of stock investment under stock price drop, the escape time is employed to represent the time of the stock price from the maximum to minimum. Also, to investigate statistical performance of the absolute and relative TTRs, we plot probability density functions of the escape time $T_{\max-\min}$ and the relative escape time ratio $R_{\max-\min}$, which indicate that the PDFs computed by using the frequency method and the kernel density estimation method are consistent. The empirical results show that increasing the data window length $N_{\max-\min}$ weakens the absolute TTR and the stability, but enhances the relative TTR; a maximum stability of the relative TTR is related to an optimal data window length; there is a peak distribution for shorter trading days and two-peak distribution for longer trading days; the absolute and relative TTRs are enhanced for the ˆDJI data but weakened for the CSI300 data as increasing trading days; the maximum stability of the absolute and relative TTRs is consistent with the optimal trading days for the ˆDJI data, but a minimum stability of the absolute and relative TTRs is consistent with the worst trading days for the CSI300 data.

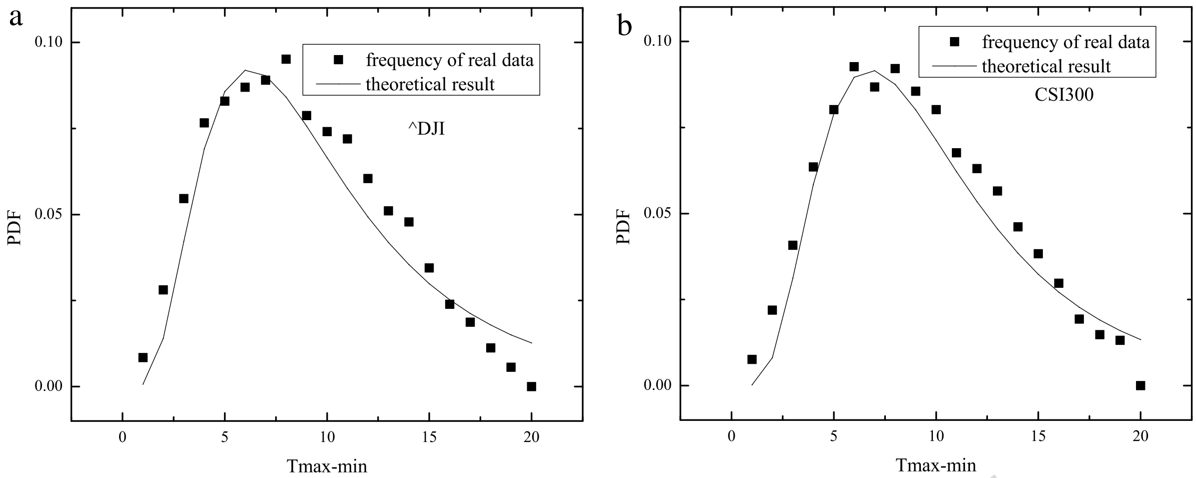

Fig. 8. Comparison of probability density functions (PDFs) of escape time $T_{max-min}$ for frequency estimation of real data and theoretical result with 1 trading day and $N_{max-min} = 20$ being the data period for the ˆDJI data in (a) and CSI300 data (b).

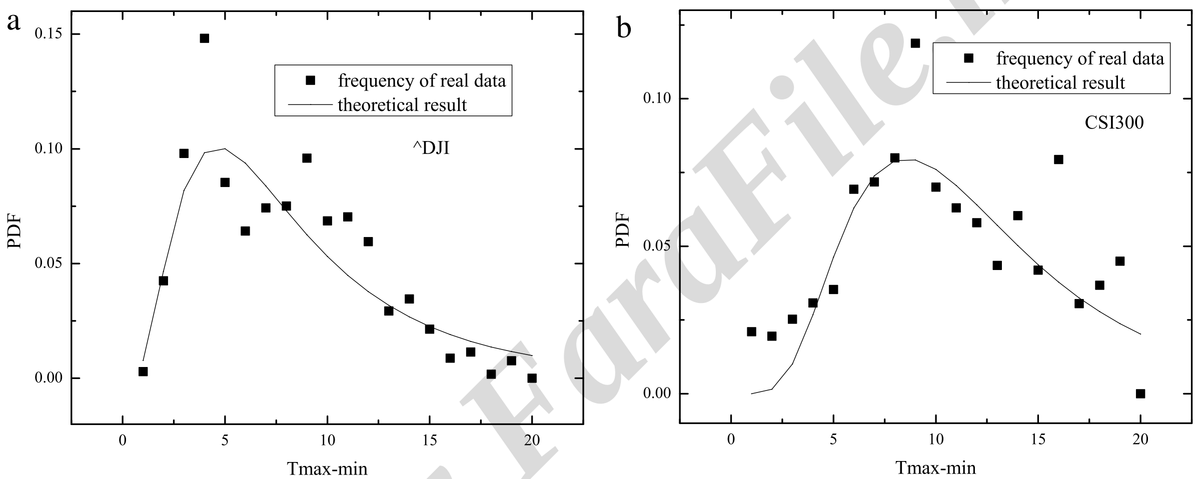

Fig. 9. Comparison of probability density functions (PDFs) of escape time $T_{max-min}$ for frequency estimation of real data and theoretical result with 30 trading days and $N_{max-min} = 20$ being the data period for the ˆDJI data in (a) and CSI300 data (b).

References

[1] P.W. Anderson, K.J. Arrow, D. Pines, The Economy as an Evolving Complex System, Addison Wesley Longman, 1988; P.W. Anderson, K.J. Arrow, D. Pines, The Economy as an Evolving Complex System II, Addison Wesley Longman, 1997.
[2] R.N. Mantegna, H.E. Stanley, An Introduction to Econophysics: Correlations and Complexity in Finance, Cambridge University Press, Cambridge, 2000.
[3] J.P. Bouchaud, M. Potters, Theory of Financial Risks, Cambridge University Press, Cambridge, 2000.
[4] J. Voit, The Statistical Mechanics of Financial Markets, Springer, Berlin, 2001.
[5] M.M. Dacorogna, R. Gencay, U.A. Müller, R.B. Olsen, O.V. Pictet, An Introduction to High-Frequency Finance, Academic Press, New York, 2001.
[6] P. Gopikrishnan, V. Plerou, L.A.N. Amaral, M. Meyer, H.E. Stanley, Scaling of the distribution of fluctuations of financial market indices, Phys. Rev. E 60 (1999) 5305.
[7] Y. Malevergne, V. Pisarenko, D. Sornette, Quant. Finance 5 (2005) 379.
[8] R.N. Mantegna, H.E. Stanley, Nature 383 (1996) 587.
[9] E.E. Peters, Chaos and Order in the Capital Markets: A New View of Cycles, Prices, and Market Volatility, John Wiley & Sons, 1996, p. 1.
[10] E.F. Fama, Efficient capital markets: A review of theory and empirical work, J. Finance 25 (1970) 383.
[11] J.P. Bouchaud, M. Potters, M. Meyer, Apparent multifractality in financial time series, Eur. Phys. J. B 13 (2000) 595.
[12] B.B. Mandelbrot, A MultifractalWalkdown, Sci. Am. 71 (1999).
[13] Z.Q. Jiang, W.X. Zhou, Multifractal analysis of Chinese stock volatilities based on the partition function approach, Physica A 387 (2008) 4881.
[14] Y. Yuan, X.T. Zhuang, Multifractal description of stock price index fluctuation using a quadratic function fitting, Physica A 387 (2008) 511.
[15] J. Huang, Experimental econophysics: Complexity, self-organization, and emergent properties, Phys. Rep. (2014).
[16] C.H. Zeng, et al., Eur. Phys. J. B 87 (2014) 1–9.
[17] T. Yang, et al., Eur. Phys. J. B 87 (2014) 1–11.
[18] T. Yang, et al., J. Stat. Mech. Theory Exp. 12 (12) (2014) P12015.
[19] Q. Han, et al., Physica A 408 (2014) 96–105.
[20] A.A. Dubkov, N.V. Agudov, B. Spagnolo, Phys. Rev. E 69 (2004) 061103-1–061103-7.
[21] B. Spagnolo, N.V. Agudov, A.A. Dubkov, Acta Phys. Pol. 35 (2004) 1419–1436.
[22] B. Spagnolo, et al., Acta Phys. Pol. 38 (2007) 1925–1950.

[23] C. Zhang, et al., Physica A 434 (2015) 68–83.
[24] C.H. Zeng, C. Zhang, J.K. Zeng, R.F. Liu, H. Wang, J. Stat. Mech. Theory Exp. 2015 (2015) P08027.
[25] C.H. Zeng, et al., Ecol. Complex. 22 (2015) 102–108.
[26] J.P. Bouchaud, R. Cont, Eur. Phys. J. B 6 (1998) 543.
[27] D. Valenti, B. Spagnolo, G. Bonanno, Physica A 382 (2007) 311.
[28] B. Spagnolo, D. Valenti, Int. J. Bifurcation Chaos 18 (2008) 2775.
[29] J. Masoliver, J. Perelló, Phys. Rev. E 78 (2008) 056104.
[30] J. Masoliver, J. Perelló, Phys. Rev. E 80 (2009) 016108.
[31] G. Bonanno, D. Valenti, B. Spagnolo, Eur. Phys. J. B 53 (2006) 405.
[32] G. Bonanno, D. Valenti, B. Spagnolo, Phys. Rev. E 75 (2007) 016106.
[33] G. Bonanno, B. Spagnolo, Fluctuation and noise letters 5 (2005) L325–L330.
[34] J.C. Li, D.C. Mei, Phys. Lett. A 377 (2013) 663.
[35] J.C. Li, C. Long, X.D. Chen, Physica A 427 (2015) 282.
[36] H. Markowitz, J. Finance 7 (1) (1952) 77–91.
[37] H.M. Markowitz, Mean-Variance Analysis in Portfolio Choice and Capital markets, Basil Blackwell, Cambridge, MA, 1987.
[38] C.M. Turner, R. Startz, C.R. Nelson, J. Financ. Econ. 25 (1989) 3.
[39] A.W. Lo, D.V. Repin, J. Cogn. Neurosci. 14 (2002) 323.
[40] Q. Tang, G. Tsitsiashvili, Stochastic Process. Appl. 108 (2003) 299.
[41] P.F. Christoffersen, Elements of Financial Risk Management, Academic Press, 2011.
[42] Yahoo Finance, http://finance.yahoo.com/q/cp?s=%5EDJI.
[43] Wind-database, http://www.wind.com.cn/En/Default.aspx.
[44] S.J. Sheather, M.C. Jones, J. R. Stat. Soc. Ser. B Stat. Methodol. 683 (1991).
[45] P. Hall, S.J. Sheather, M. Jones, J. Marron, Biometrika 78 (1991) 263.
[46] S.T. Chiu, Ann. Statist. 1883 (1991).
[47] H. Lévy, H.M. Markowitz, Amer. Econ. Rev. 69 (1979) 308–317.
[48] P. Gopikrishnan, M. Meyer, L.A.N. Amaral, H.E. Stanley, Eur. Phys. J. B 3 (1998) 139.
[49] F. Lillo, R.N. Mantegna, Phys. Rev. E 62 (2000) 6126.
[50] A.A. Drăgulescu, V.M. Yakovenko, Quant. Finance 2 (2002) 443.
[51] A.C. Silva, V.M. Yakovenko, Physica A 324 (2003) 303.